*J Appl Physiol*
89: 1636–1644, 2000.

cutting-edge report

# Wave-intensity analysis: a new approach to coronary hemodynamics

YI-HUI SUN,[1] TODD J. ANDERSON,[1] KIM H. PARKER,[2] AND JOHN V. TYBERG[1]
[1]*Departments of Medicine and Physiology and Biophysics, University of Calgary, Calgary, Alberta, Canada T2N 4N1; and* [2]*Physiological Flow Studies Group, Department of Biological and Medical Systems, Imperial College of Science, Technology, and Medicine, London SW7 2BY, United Kingdom*

Received 15 March 2000; accepted in final form 20 April 2000

**Sun, Yi-Hui, Todd J. Anderson, Kim H. Parker, and John V. Tyberg.** Wave-intensity analysis: a new approach to coronary hemodynamics. *J Appl Physiol* 89: 1636–1644, 2000.—In 10 anesthetized dogs, we measured high-fidelity left circumflex coronary ($P_{LCx}$), aortic ($P_{Ao}$), and left ventricular ($P_{LV}$) pressures and left circumflex velocity ($U_{LCx}$; Doppler) and used wave-intensity analysis (WIA) to identify the determinants of $P_{LCx}$ and $U_{LCx}$. Dogs were paced from the right atrium (*control 1*) or right ventricle by use of single (*control 2*) and then paired pacing to evaluate the effects of left ventricular contraction on $P_{LCx}$ and $U_{LCx}$. During left ventricular isovolumic contraction, $P_{LCx}$ exceeded $P_{Ao}$, paired pacing increasing the difference. Paired pacing increased $\Delta P_X$ (the $P_{LCx}$-$P_{Ao}$ difference at the $P_{Ao}$-$P_{LV}$ crossover) and average $dP_{LCx}/dt$ ($P < 0.0001$ for both). During this time, WIA identified a backward-going compression wave (BCW) that increased $P_{LCx}$ and decreased $U_{LCx}$; the BCW increased during paired pacing ($P < 0.0001$). After the aortic valve opened, the increase in $P_{Ao}$ caused a forward-going compression wave that, when it exceeded the BCW, caused $U_{LCx}$ to increase, despite $P_{LV}$ and (presumably) elastance continuing to increase. Thus WIA identifies the contributions of upstream (aortic) and downstream (microcirculatory) effects on $P_{LCx}$ and $U_{LCx}$.

coronary blood flow; hemodynamics; contraction; relaxation

ALTHOUGH AORTIC PRESSURE ($P_{Ao}$) is the main determinant of coronary arterial pressure and flow, it is clear that coronary arterial pressure and flow are not simple functions of $P_{Ao}$ (15). The coronary circulation is particularly complicated, in that blood flows through the myocardium, which, as it contracts, increasingly impedes flow. In the arteries perfusing the left ventricle (LV), systolic coronary flow is small compared with diastolic flow (5–7, 27, 30), in contradistinction to those arteries perfusing the right ventricle, in which maximal flow occurs during systole (3). [That systolic flow is small in large coronary arteries is related to the fact that flow reverses in the penetrating arteries (4), that subendocardial flow is retrograde (8), and that the capacitance of large epicardial coronary arteries is substantial (4).] The mechanisms by which LV contraction impedes left coronary blood flow have been studied for many years. The "vascular waterfall" (7) and the "intramyocardial pump" models (30) have been used to explain how increasing intramyocardial pressure impedes coronary blood flow during systole. Using a "time-varying elastance" model, Krams and colleagues (16) explained how systolic flow is impeded by changes in extravascular stiffness that result from contraction of the fibers surrounding intramyocardial blood vessels.

These models explain the early-systolic decrease in coronary blood flow, but they do have limitations. First, they cannot explain the increase in coronary blood flow (4) that occurs after the initial minimum, despite the continuing increase in intramyocardial pressure and myocardial elastance. Second, because perfusion pressure was held constant in many previous studies, the results of those studies might not apply to physiological conditions when coronary pressure and flow vary throughout a cardiac cycle. Furthermore, coronary pressure and flow are determined by *1*) upstream aortic effects, which are related to LV function and the properties of the systemic circulation, and *2*) downstream microcirculatory effects, which are also related. Changes in LV function (e.g., changes in contractility) will affect coronary perfusion pressure and myocardial compressive force, and results from studies using constant perfusion pressure and maximal coronary vasodilation may over- or underestimate the effects of contractility on coronary blood flow.

Address for reprint requests and other correspondence: J. V. Tyberg, Dept. of Medicine and Physiology and Biophysics, University of Calgary, Health Sciences Centre, 3330 Hospital Dr. NW, Calgary, AB, Canada T2N 4N1 (E-mail: jtyberg@ucalgary.ca).

The costs of publication of this article were defrayed in part by the payment of page charges. The article must therefore be hereby marked "*advertisement*" in accordance with 18 U.S.C. Section 1734 solely to indicate this fact.

 8750-7587/00 $5.00 Copyright © 2000 the American Physiological Society 

Therefore, because of the need to identify and quantitate upstream and downstream effects, we employed wave-intensity analysis (WIA), a time-domain analysis introduced by Parker and colleagues (13, 22, 23). [Recently, WIA was employed to elucidate the dynamics of pulmonary venous flow (29) and, in the neonate, pulmonary arterial pressure (10).] On the basis of measurements of left coronary arterial pressure and velocity, WIA can discriminate downstream from upstream events and represent their interaction.

The purposes of the present study were *1*) to clarify the dynamic pressure and velocity characteristics of the distal LV coronary circulation and *2*) to provide a mechanistic explanation for acceleration and deceleration of coronary flow with use of WIA.

*Glossary*

| | |
|---|---|
| $c$ | Wave speed |
| $dI_W$ | Net intensity (formerly called dPd$U$) |
| $dI_{W^+}$ | Intensity of a forward-going wave |
| $dI_{W^-}$ | Intensity of a backward-going wave |
| dP | Incremental change in pressure during the sampling interval at any time and location |
| $dP_+$ | Difference in pressure across a forward-going wave |
| $dP_-$ | Difference in pressure across a backward-going wave |
| d$U$ | Incremental change in velocity during the sampling interval at any time and location |
| $I_{W^+}$ | Energy of a forward-going wave |
| $I_{W^-}$ | Energy of a backward-going wave |
| LCx | Left circumflex coronary artery |
| LV | Left ventricle (ventricular) |
| P | Pressure |
| ρ | Density |
| $U$ | Velocity |
| WIA | Wave-intensity analysis |

## METHODS

*Instrumentation.* The studies were performed on 10 18- to 20-kg mongrel dogs of either gender. Dogs were anesthetized with thiopental sodium and then with fentanyl citrate and ventilated with a constant-volume respirator to maintain normal blood gas tensions and pH. The pericardium was opened along the atrioventricular groove. $P_{Ao}$ and LV pressure ($P_{LV}$) were measured using catheter-tipped manometers

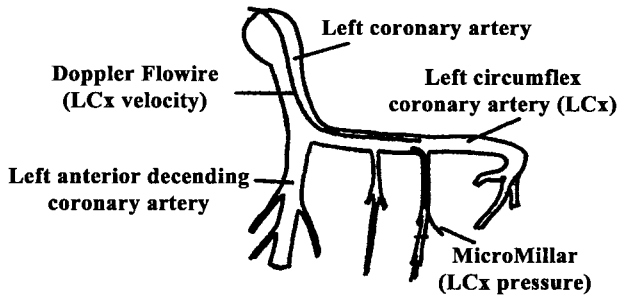


Fig. 1. Schematic diagram of the placement of the catheter-tipped pressure transducer and the Doppler Flowire within the distal left circumflex coronary artery (LCx). Pressure and velocity were measured at the same location.

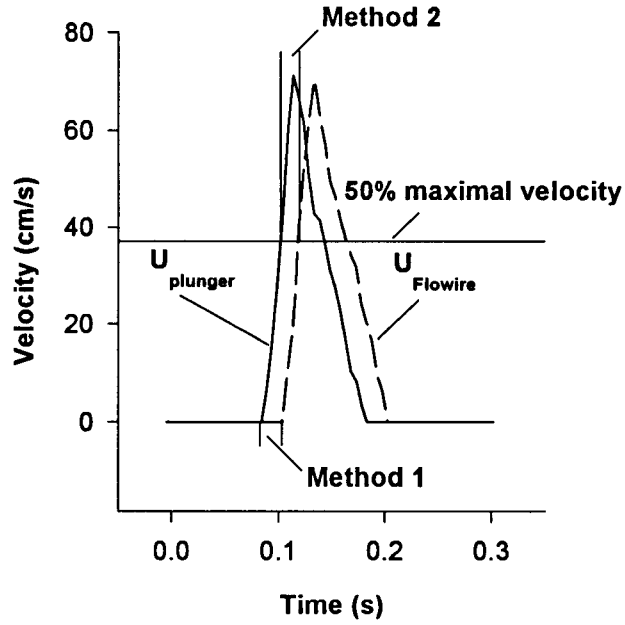


Fig. 2. Determination of delay time of Doppler Flowire. A foot-to-foot method (*method 1*) or a 50% maximum method (*method 2*) was used to compare velocity of the syringe plunger ($U_{plunger}$) with velocity of the water ($U_{Flowire}$).

(Millar Instruments, Houston, TX) inserted via the right femoral and left carotid arteries, respectively. The catheter-tipped manometers in the aorta (just beyond the aortic valve) and LV were referenced via their fluid-filled lumens so that absolute values of pressure could be ascertained. All pressures were referenced to the midplane of the LV. A pneumatic constrictor (In Vivo Metrics, Healdsburg, CA) was placed around the inferior vena cava. After cardiac instrumentation, the pericardium was reapproximated by single interrupted sutures.

As illustrated in Fig. 1, we introduced a 2.5-F catheter-tipped manometer (Millar Instruments) into a 1.0- to 1.5-mm LCx branch and advanced it retrogradely 3 mm into the LCx coronary artery to record $P_{LCx}$. A Doppler Flowire was introduced (via the left femoral artery) under fluoroscopic observation to measure LCx velocity ($U_{LCx}$) at the same location at which pressure was measured. Because the LCx branch was too small to accommodate a catheter with a lumen, the absolute value of $P_{LCx}$ could not be ascertained in the same manner as $P_{LV}$, for example. Because we determined that wave intensity was negligible during an interval preceding LV end diastole, we assumed that $P_{LCx}$ was then equal to $P_{Ao}$ and matched $P_{LCx}$ to $P_{Ao}$ at end diastole. (In addition, in a series of 3 other dogs, we used a fine plastic tube and a conventional pressure transducer to record $P_{LCx}$ and found that $P_{LCx}$ was indeed equal to $P_{Ao}$ before end diastole.) A pair of ultrasonic crystals was implanted in the anterior midwall of the LV to measure a circumferential segment length ($L_{LV}$). Pacing wires were attached to the right atrium and to the right ventricular free wall to control heart rate and to effect paired pacing.

*Doppler delay.* Using a linear potentiometer to measure the position of the plunger of a 5-ml syringe (11), we compared the differentiated position signal with fluid velocity as measured using a Doppler Flowire (Cardiometrics, Mountainview, CA). We measured the delay by a foot-to-foot method (*method 1*) and a 50% maximum method (*method 2;* Fig. 2). Forty-nine observations were analyzed.

Table 1. *Nomenclature of WIA*

| Wave | $dP_{\pm}$ | P | $U$ |
|---|---|---|---|
| FCW | $dP_+ > 0$ | ↑ | ↑ |
| BCW | $dP_- > 0$ | ↑ | ↓ |
| FEW | $dP_+ < 0$ | ↓ | ↓ |
| BEW | $dP_- < 0$ | ↓ | ↑ |

WIA, wave-intensity analysis; $dP_{\pm}$, pressure difference across a forward- or backward-going wave front; P, effect of the wave on pressure; $U$, effect of the wave on velocity in the direction of net blood flow; FCW, forward-going compression wave; $dP_+$, pressure difference across a forward-going wave front; BCW, backward-going compression wave; $dP_-$, pressure difference across a backward-going wave front; FEW, forward-going expansion wave; BEW, backward-going expansion wave.

*Protocols.* After instrumentation and a 15- to 20-min stabilization interval, all hemodynamic data ($P_{LV}$, $P_{LCx}$, $P_{Ao}$, $U_{LCx}$, and $L_{LV}$) were recorded while the heart was paced from the right atrium (*control 1*). A second set of control data (*control 2*) was recorded while the heart was paced from the right ventricle with single stimuli. Finally, paired pacing data were recorded while the heart was paced from the right ventricle with paired stimuli to increase contractility (25). Using $P_{LV}$-$L_{LV}$ loops described during caval constriction under *control 2* and paired-pacing conditions, we defined a linear end-systolic $P_{LV}$-$L_{LV}$ relation, the slope of which [maximal elastance ($E_{max}$)] was taken as a measure of contractility. Individual hearts were paced at the same rate in *control 1, control 2*, and paired-pacing conditions. Among the different dogs, heart rate ranged from 85 to 100 $min^{-1}$. All the hemodynamic data were sampled at ~200 Hz and recorded using a computer system (Sonometrics, London, ON, Canada).

*WIA.* WIA was used to identify and quantitate upstream (aortic) and downstream (coronary microcirculatory) events and their interaction. WIA provides information regarding the direction, intensity, and type of waves present at any given moment and location in a blood vessel (12, 22, 23). Because WIA is a time-domain analysis, wave intensity can be related temporally to hemodynamic parameters and beat-to-beat analyses can be performed (13, 22). WIA was developed by solving nonlinear one-dimensional equations of motion and is based on the concept that "waves" (i.e., propagated disturbances) that travel through the vasculature are manifested by changes in pressure and velocity (23). The energy that is transported by a wave can be quantified by measuring the changes in pressure and velocity across the wave front (19). Waves can be forward going (i.e., in the direction of net blood flow) or backward going in direction and compression or expansion in type. Thus there are four possible combinations: forward-compression, backward-compression, forward-expansion, and backward-expansion (Table 1). Compression waves have a "pushing" effect and increase pressure. Forward-going compression waves increase pressure and increase velocity, whereas backward-going compression waves increase pressure and decrease velocity (in the forward direction). Expansion waves have a "pulling" effect and decrease pressure. Forward-going expansion waves decrease pressure and decrease velocity, whereas backward-going expansion waves decrease pressure and increase velocity (in the forward direction).

To determine whether a wave is a compression or an expansion wave, we calculate the pressure differences across the wave front. The pressure differences across the wave fronts of forward-going waves ($dP_+$; e.g., those from the upstream aorta) and across the wave fronts of backward-going waves ($dP_-$; e.g., those from the downstream coronary microcirculation) are calculated as

$$dP_+ = (½)(dP + \rho c\, dU)$$

$$dP_- = (½)(dP - \rho c\, dU)$$

where $\rho$ is the density of blood, $c$ is the wave speed, dP is the incremental difference in $P_{LCx}$, and $dU$ is the incremental difference in $U_{LCx}$ during a sampling interval (~0.005 s). [At any location, the measured change in pressure (dP) is the sum of $dP_+$ and $dP_-$.] Because $c$ cannot be determined when forward and backward waves are simultaneously present, $c$ was calculated as the absolute value of $dP/\rho dU$ (23) at the beginning of systole, when we were confident that only a backward-going wave was present [$c$ was between 5.3 and 7.9 m/s, values consistent with earlier measurements by other methods (2, 9, 26)]. The sign of the pressure gradient across a wave front ($dP_+$ or $dP_-$) determines whether the wave is a compression or an expansion wave (i.e., if $dP_+ > 0$, the forward-going wave is a compression wave, and if $dP_+ < 0$, it is an expansion wave; if $dP_- > 0$, the backward-going wave is a compression wave, and if $dP_- < 0$, it is an expansion wave).

The intensities of the forward-going ($dI_{W^+}$) and backward-going ($dI_{W^-}$) waves are expressed in units of normalized power ($W/m^2$). At any instant, the algebraic sum of $dI_{W^+}$ and $dI_{W^-}$ is the net intensity ($dI_W$; formerly dPdU). These quantities are calculated as follows

$$dI_{W^+} = (¼\,\rho c)(dP + \rho c\, dU)^2$$

$$dI_{W^-} = (-¼\,\rho c)(dP - \rho c\, dU)^2$$

$$dI_W = dI_{W^+} + dI_{W^-} = dP\,dU$$

$dI_{W^+}$ and $dI_{W^-}$ directly represent the respective effects of the upstream aorta and the downstream coronary microcirculation at any location. When $dI_W$ is positive ($dI_W > 0$), the forward-going wave (i.e., the aortic effect) is dominant; when $dI_W$ is negative ($dI_W < 0$), the backward-going wave (i.e., the coronary microcirculatory effect) is dominant. If the values of $dI_{W^+}$ and $dI_{W^-}$ are similar or very small in magnitude, $dI_W$ will be very small.

Energy ($J/m^2$) of the forward-going ($I_{W^+}$) or backward-going ($I_{W^-}$) wave was calculated by integrating the area under the respective intensity waveform

$$I_{W^+} = \int (dI_{W^+})dt$$

$$I_{W^-} = \int (dI_{W^-})dt$$

*Data analysis.* Using specialized software (CVSOFT, Odessa Computer Systems, Calgary, AB, Canada), we calculated dP and $dU$, the incremental difference in $P_{LCx}$ and $U_{LCx}$ during a sampling interval from measured $P_{LCx}$ and $U_{LCx}$. $dI_{W^+}$, $dI_{W^-}$, $dI_W$, $I_{W^+}$, and $I_{W^-}$ were calculated as described above. On the basis of Doppler delay measurements (see below) and as confirmed by the manufacturer, we advanced all the Doppler Flowire data 20 ms in time.

As a measure of the effect of LV systolic contraction on $P_{LCx}$, the pressure difference between $P_{LCx}$ and $P_{Ao}$ ($\Delta P_X$) was calculated at the $P_{Ao}$-$P_{LV}$ crossover, as shown in Figs. 3 and 4. Also, $I_{W^-}$ was measured, and the slopes of the $P_{LCx}$ and $P_{Ao}$ waveforms were approximated during isovolumic contraction, the interval between end diastole and the $P_{Ao}$-$P_{LV}$ crossover, before and after contractility was increased by paired pacing. [The slopes, $dP_{LCx}/dt$ and $dP_{Ao}/dt$, were approximated by taking the values of the slopes of straight-line segments drawn between the point of divergence (i.e., end diastole) and the $P_{Ao}$-$P_{LV}$ crossover.] Because it was difficult to ascertain the absolute value of $P_{LCx}$ and because the time

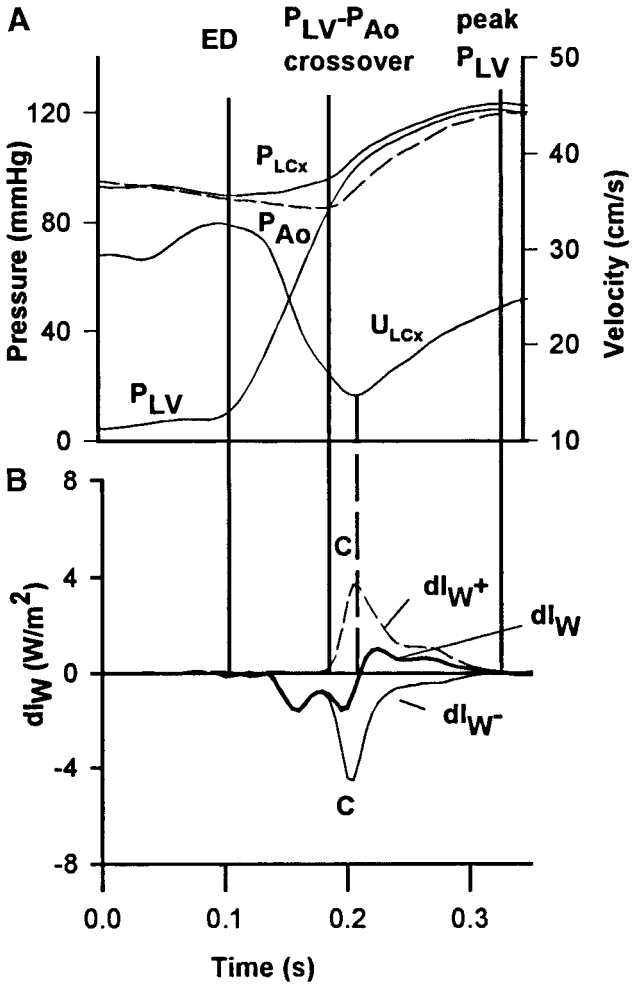


Fig. 3. *A*: left ventricular pressure ($P_{LV}$), aortic pressure ($P_{Ao}$, dashed line), LCx pressure ($P_{LCx}$), and LCx velocity ($U_{LCx}$) waveforms during an early-systolic interval of a representative cardiac cycle. *B*: backward intensity ($dI_{W^-}$, light solid line), forward intensity ($dI_{W^+}$, dashed line), and net wave intensity ($dI_W$, heavy solid line) waveforms. C, compression wave. Solid vertical lines indicate end diastole (ED), the instant at which $P_{LV}$ exceeds $P_{Ao}$ (i.e., the $P_{LV}$-$P_{Ao}$ crossover), and the time at which $P_{LV}$ achieves its peak value. Dashed vertical line, $U_{LCx}$ minimum.

derivatives are independent of the absolute values of pressure, $dP_{LCx}/dt$ and $dP_{Ao}/dt$ were compared to determine whether paired pacing increased the divergence of $P_{LCx}$ and $P_{Ao}$.

*Statistics.* Under each condition (*control 1, control 2*, and paired pacing), 10 cardiac cycles were randomly selected and the average values were obtained. Results from the 10 dogs are expressed as means ± SD. Student's paired *t*-test was used to identify statistically significant differences; $P < 0.05$ was considered significant.

## RESULTS

*Measurement of Doppler delay.* According to *method 1* (Fig. 2), the mean delay was 22.7 ± 0.6 ms and the median was 22.9 ms. According to *method 2*, the mean delay was 22.0 ± 0.8 ms and the median was 21.7 ms.

*Net wave intensity.* Figure 5 indicates the changes in coronary net wave intensity during a typical cardiac cycle. Between end diastole and the moment that $U_{LCx}$ reached a minimum, a backward-going compression wave was dominant, which was associated with increasing $P_{LCx}$ and decreasing $U_{LCx}$. Between the $U_{LCx}$ minimum and the moment that $P_{LCx}$ reaches a maximum, a forward-going compression wave was dominant, which was associated with a further increase in $P_{LCx}$ and increasing $U_{LCx}$. Later, during LV relaxation, a forward-going expansion wave developed and became dominant until the aortic valve closed at the incisura. This expansion wave was associated with decreases in $P_{LCx}$ and $U_{LCx}$. At the incisura, there was a brief, dominant, forward-going compression wave that was associated with increases in $P_{LCx}$ and $U_{LCx}$. As LV relaxation continued, however, a backward-going expansion wave that was associated with decreased $P_{LCx}$ and increased $U_{LCx}$ became dominant.

*Intensity of forward- and backward-going waves during LV contraction.* Figure 3 illustrates early systolic events in detail. Figure 3*A* shows how $P_{LCx}$ differs from $P_{Ao}$. Diastolic $P_{Ao}$ fell monotonically until it was exceeded by $P_{LV}$ (i.e., at the $P_{Ao}$-$P_{LV}$ crossover). From middiastole, distal $P_{LCx}$ was identical to $P_{Ao}$ but, at the beginning of LV isovolumic contraction (i.e., at end diastole), $P_{LCx}$ stopped falling. Thereafter, it remained constant or began to increase somewhat, but in either case it exceeded $P_{Ao}$ until near the end of LV ejection.

As shown in Fig. 3*B*, we used WIA to clarify the mechanism that caused this difference between $P_{LCx}$ and $P_{Ao}$. Immediately after LV end diastole, a backward-going compression wave was generated, and after the opening of the aortic valve, a forward-going compression wave was generated. $dI_{W^-}$ started to increase (in absolute magnitude) after end diastole, achieved its peak during early LV ejection, and returned to zero approximately at the time $P_{LV}$ reached its peak. $dI_{W^+}$ started to increase at the beginning of

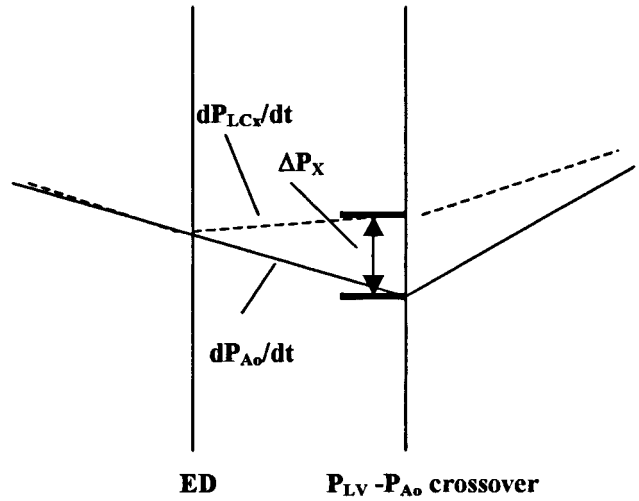


Fig. 4. An idealized magnification of coronary pressure and $P_{Ao}$ during isovolumic contraction (cf. Fig. 3) illustrates how we measured the effects of LV systolic contraction on coronary pressure. The 2 vertical lines indicate end-diastole (ED) and the moment at which the $P_{LV}$-$P_{Ao}$ crossover occurred; $\Delta P_X$ indicates the $P_{LCx}$-$P_{Ao}$ pressure difference at that moment. $dP_{LCx}/dt$ and $dP_{Ao}/dt$, average slopes of $P_{LCx}$ and $P_{Ao}$ during the isovolumic interval.

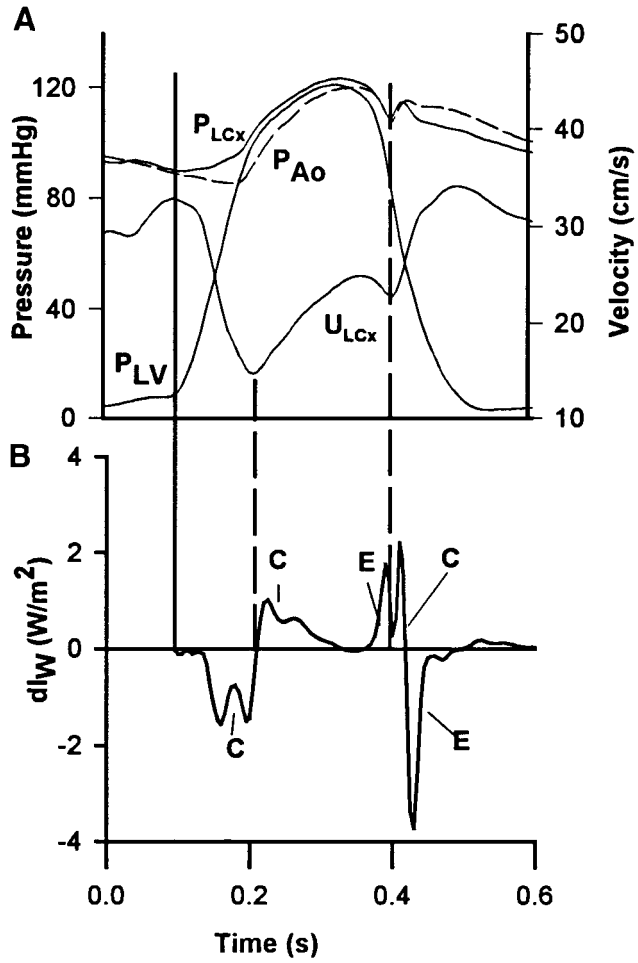


Fig. 5. *A*: $P_{LV}$, $P_{Ao}$ (dashed line), $P_{LCx}$, and $U_{LCx}$ waveforms during a representative cardiac cycle. *B*: net wave intensity ($dI_W$) waveform. C, compression wave; E, expansion wave. Solid vertical line, end diastole (ED); dashed vertical lines, $U_{LCx}$ minima.

ejection, and although it increased rapidly, its absolute magnitude did not become greater than that of $dI_{W^-}$ until after ~25 ms (i.e., the point at which $dI_W$ became positive). It also returned to zero when $P_{LV}$ reached its maximum value.

*Effects of paired pacing.* During *control 1*, $\Delta P_X$ was 4.3 ± 2.5 mmHg, which doubled during paired pacing ($P < 0.0001$), an intervention that increased $E_{max}$ (i.e., contractility) almost threefold (Table 2). During the isovolumic contraction interval, $dP_{Ao}/dt$ was −53.9 ± 19.5 mmHg/s during *control 1* and did not change with paired pacing. $dP_{LCx}/dt$ was 3.4 ± 4.4 during *control 1* ($P < 0.0001$ vs. $dP_{Ao}/dt$) and increased to 142 ± 25 mmHg/s during paired pacing ($P < 0.0001$). As shown in Table 2, paired pacing increased the peak value of $dI_{W^-}$ by a factor of ~3 and $I_{W^-}$ by a factor of ~4. (There were no significant differences between data obtained during *control 1* and *control 2*.)

*Intensity of forward- and backward-going waves during LV relaxation.* As illustrated in Fig. 6, after the beginning of LV relaxation and the beginning of the decrease in $P_{LCx}$, forward and backward expansion waves began to be generated. Typically, relaxation was characterized by triplets of forward and backward waves. The forward and backward expansion waves in late systole were followed by forward and backward compression waves temporally related to aortic valve closure, after which there were paired forward and backward expansion waves.

## DISCUSSION

Among the systemic circulations, the LV coronary circulation is particularly complicated, because its driving force and impedance to flow are dynamic functions of contraction. LV contraction not only increases coronary perfusion pressure but, several milliseconds earlier at end diastole, begins to increase the compression of the microcirculation. LV relaxation not only decreases coronary perfusion pressure but decreases the compression of the microcirculation. Therefore, coronary blood velocity is determined by upstream (aortic) and downstream (microcirculatory) events. Compared with previous approaches, the salient advantage of WIA is that it provides information about upstream and downstream events in the time domain and, therefore, on a beat-to-beat basis, provides direct information about the interaction of the upstream and downstream effects.

From the outset, it should be made clear that our WIA approach to waves in the arteries is fundamentally different from those approaches that are based on Fourier analysis. Fourier analysis is based on the observation that any periodic waveform can be expressed as the summation of sinusoidal waves of different frequencies (harmonics), each with the appropriate amplitude and phase. These sinusoidal wave trains are the fundamental basis of any Fourier technique, an

Table 2. *Coronary-aortic pressure differences during isovolumic contraction and effects of paired pacing*

| | $E_{max}$, mmHg/mm | $dI_{W^-}$, W/m$^2$ | $I_{W^-}$, J/m$^2$ | $\Delta P_X$, mmHg | $dP_{Ao}/dt$, mmHg/s | $dP_{LCx}/dt$, mmHg/s |
|---|---|---|---|---|---|---|
| *Control 1* (RA single pacing) | 34.2 ± 8.5 | 0.20 ± 0.08 | 12.4 ± 4.7 | 4.3 ± 2.5 | −53.9 ± 19.5 | 3.4 ± 4.4† |
| *Control 2* (RV single pacing) | 36.6 ± 10.6 | 0.23 ± 0.09 | 13.9 ± 5.2 | 4.5 ± 2.0 | −48.4 ± 23.3 | 3.8 ± 5.0† |
| Paired pacing (RV) | 93.6 ± 20.7* | 0.78 ± 0.21* | 46.8 ± 12.8* | 9.1 ± 3.8* | −67.4 ± 20.3 | 142.1 ± 25.1*† |

Values are means ± SD. $E_{max}$, maximum, end-systolic value of elastance (i.e., contractility); $dI_{W^-}$, peak value of the intensity (power) of the backward-going compression wave; $I_{W^-}$, time-integral (energy) of the backward-going compression wave; $\Delta P_X$, difference between left circumflex coronary artery pressure ($P_{LCx}$) and aortic pressure ($P_{Ao}$) at the $P_{Ao} - P_{LV}$ crossover; $P_{Ao}/dt$ and $dP_{LCx}/dt$, slopes of $P_{Ao}$ and $P_{LCx}$ vs. time during isovolumic contraction. *$P < 0.0001$ vs. *control 2*; †$P < 0.0001$ vs. $dP_{Ao}/dt$.

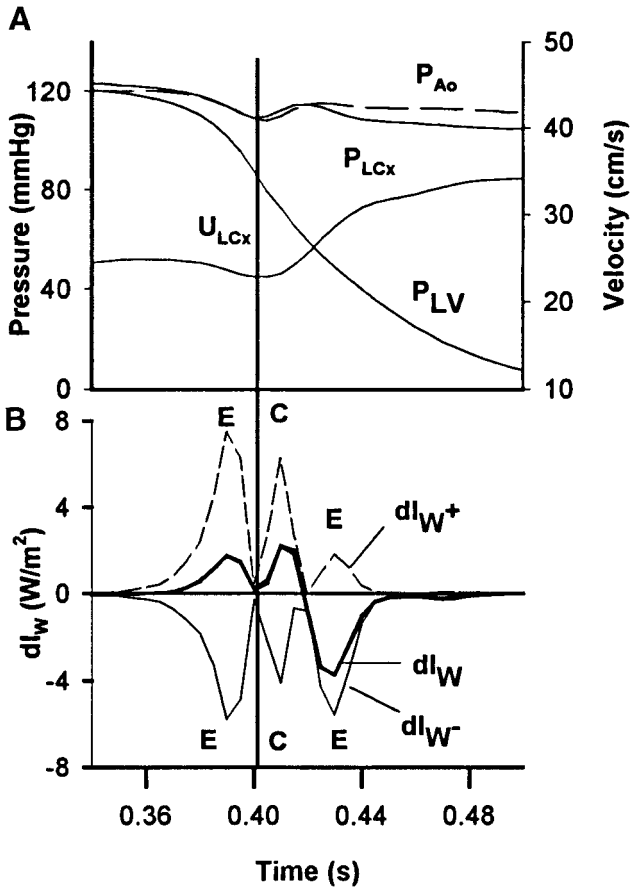


Fig. 6. *A*: $P_{LV}$, $P_{Ao}$ (dashed line), $P_{LCx}$, and $U_{LCx}$ waveforms during early relaxation of a representative LV cycle. *B*: backward intensity ($dI_{W^-}$, light solid line), forward intensity ($dI_{W^+}$, dashed line), and net wave intensity ($dI_W$, heavy solid line). E, expansion wave; C, compression wave.

archetypal example being the synthesis of speech from different sinusoidal tones.

An alternative approach to waves, WIA, is to consider the propagation of individual wave fronts characterized by a change in pressure, dP, and velocity, d$U$. An example of this type of wave is the "bore" seen in some river estuaries, notably the Severn, where a single wave front generated by the tide propagates up the river. It is convenient to consider small, infinitesimal wave fronts as the fundamental elements of our analysis, since any finite waveform can be constructed from a sequence of individual wave fronts of the appropriate magnitude. For example, any waveform sampled at uniform intervals can be thought of as the summation of the changes between successive samples. This approach to the synthesis of a finite waveform has the advantage that it does not make any assumptions about periodicity and can therefore be applied to transient and periodic waveforms. Beat-to-beat analysis is amenable to WIA, whereas it is not if Fourier techniques are employed.

The pressure change across a wave front can be positive, $dP > 0$ (which defines the wave as a compression wave), or negative, $dP < 0$ (which defines it as an expansion wave). Compression waves arise from pushing or blowing, and they cause an increase of velocity in the direction of the wave. Expansion waves arise from pulling or sucking, and they cause a decrease of velocity in the direction of the wave. If we define velocity to be positive in the direction of mean blood flow, a forward-going compression wave will accelerate the blood ($dU > 0$), whereas a backward-going compression wave will decelerate the blood ($dU < 0$). Similarly, a forward-going expansion wave will decelerate the blood ($dU < 0$), whereas a backward-going expansion wave will accelerate the blood ($dU > 0$). It may be helpful to think of blood flow in a coronary artery being manipulated by two "Maxwell demons," one at the arterial end of the artery and the other at the microcirculation end. The arterial demon could accelerate coronary blood flow by blowing into his end of the artery, which would increase the pressure, which would result in a forward-going compression wave. If, however, the microcirculation demon blew into his end of the artery, the pressure would be similarly increased, creating a backward-going compression, which would decelerate the flow. If the microcirculation demon wanted to accelerate the flow, he would have to suck on the artery, thereby decreasing the pressure. Simply measuring the change in pressure at some point in the artery cannot reveal the direction of travel of the wave front causing the change in pressure. To do this, it is necessary to simultaneously measure the change in velocity. If, however, there are simultaneous forward and backward waves, as is generally the case in the coronary arteries, then further analysis of the measured dP and d$U$ is necessary to distinguish the properties of the two waves. WIA allows us to do this.

Between end diastole and the moment that $U_{LCx}$ reached a minimum, LV contraction generated a dominant, backward-going compression wave, which had the effect of increasing $P_{LCx}$ and decreasing $U_{LCx}$ (Fig. 5). (The compression of the vasculature resulted in a "pushing" effect that traveled backward, against the direction of blood flow.) Between the $U_{LCx}$ minimum and the moment that $P_{LCx}$ reaches a maximum, a forward-going compression wave generated by the increasing $P_{Ao}$ became dominant, which continued to increase $P_{LCx}$ further and to increase $U_{LCx}$. (The increase in $P_{Ao}$ resulted in a pushing effect that traveled forward, in the same direction as blood flow.) Later, as the LV began to relax and $P_{Ao}$ began to fall, a forward-going expansion wave developed and became dominant until the aortic valve closed at the incisura. (The decrease in $P_{Ao}$ resulted in a "pulling" effect that traveled forward, in the same direction as blood flow.) This expansion wave decreased $P_{LCx}$ and $U_{LCx}$. Aortic closure generated a brief, dominant, forward-going compression wave that increased $P_{LCx}$ and $U_{LCx}$. As LV relaxation continued, however, a backward-going expansion wave became dominant, which decreased $P_{LCx}$ and increased $U_{LCx}$. (Decreasing LV compression resulted in a pulling effect that traveled backward, against the direction of blood flow.)

*Effects of LV contraction on coronary blood pressure and velocity.* From high-fidelity measurements of aortic and distal coronary pressure, we have demonstrated that $P_{LCx}$ is greater than $P_{Ao}$ during LV isovolumic contraction, an observation that, to our knowledge, has not been reported previously. WIA identified an early-systolic backward-going compression wave [presumably generated by the contracting myocardium, which causes retrograde subendocardial flow (4) and reverses flow in small penetrating branches (8)] that increased $P_{LCx}$ and decreased $U_{LCx}$. When LV contractility was augmented by paired pacing, the changes in coronary pressure and the changes in the backward-going compression wave were consistent: $\Delta P_X$, $dP_{LCx}/dt$, $dI_{W^-}$, and $I_{W^-}$ increased (Table 2). Westerhof and Sipkema and their colleagues (16–18, 33) related LV elastance to coronary flow impediment, we have preliminary data that demonstrate that the peak intensity of the backward compression wave is directly related to systolic coronary flow reduction (32), and Suga and Sagawa and co-workers (28, 31) equated increased myocardial elastance with increased contractility. Thus we conclude that paired pacing increased $I_{W^-}$, which caused the changes in $P_{LCx}$.

The same myocardial-compression mechanism that generates a backward-going compression wave may account, in part, for the systolic pulsations in distal coronary pressure after a coronary artery has been occluded (30). It may also account for retrograde systolic coronary flow (14), and the same phenomenon may be related to the observed systolic increase in epicardial coronary venous pressure (1). During early systole, the forward- and backward-going waves are compression waves, and, as such, both tend to increase $P_{LCx}$. We suggest that this may help explain the fact that $P_{LCx}$ continued to exceed $P_{Ao}$ after the beginning of ejection.

Although $dI_{W^+}$ and $dI_{W^-}$ usefully represent the separate upstream aortic and downstream microcirculatory effects, $dI_W$ (the net intensity) is important, because it defines the balance of upstream and downstream forces and, therefore, determines whether the blood accelerates or decelerates. Because no forward wave was identified ($dI_{W^+} = 0$) during isovolumic contraction, $dI_W = dI_{W^-}$ and the unopposed backward compression wave decreased $U_{LCx}$ and increased $P_{LCx}$ (Fig. 3). After the aortic valve opened, $dI_{W^+}$ began to increase and rapidly achieved an absolute magnitude almost as great as that of $dI_{W^-}$. However, $U_{LCx}$ began to increase only after ~25 ms. At that time, when the intensity of the forward compression wave became greater than that of the backward compression wave (i.e., the upstream aortic pushing effect became greater than that from the downstream microcirculation), $dI_W$ crossed zero and became positive and $U_{LCx}$ stopped decreasing and began to increase. Thus $dI_W$ would seem to be an indicator of the "prevailing wind," and $U_{LCx}$ changes immediately and accordingly.

After the beginning of ejection, $dI_{W^-}$ continued to increase (in absolute value). This may imply that vascular compression increased during later ejection when $P_{LV}$ continued to increase and LV volume decreased. Although increasing pressure and decreasing volume each would tend to increase $dI_{W^-}$, the increase in $dI_{W^-}$ may be best predicted by the increase in elastance (the ratio of pressure to volume).

Using a special-purpose pressure generator, Recchia et al. (24) recently showed that systolic coronary flow is markedly augmented when pulse pressure is increased. Although they have demonstrated that part of this increase is mediated by endothelium-dependent mechanisms (20, 21), it seems clear that a substantial part of the increase must be attributed to a larger forward-going compression wave caused by the augmented pulse pressure.

For decades, investigators have attempted to understand the mechanism by which the contracting LV impedes its own blood supply, and several models have been proposed to explain the decrease in coronary arterial flow in systole. The vascular waterfall model of Downey and Kirk (7) and the intramyocardial pump model of Spaan and colleagues (30) have been used to explain how increasing intramyocardial pressure (which is closely related to $P_{LV}$) impedes coronary flow. Using the time-varying elastance model, Westerhof and Sipkema and colleagues (16–18, 33) explained how systolic flow is impeded by changes in extravascular stiffness that result from contraction of the myocytes surrounding intramyocardial blood vessels. Although these models account for the early-systolic decrease in flow, in themselves they do not account for the increase in flow that occurs during ejection when intramyocardial pressure and myocardial elastance continue to increase. WIA appears to identify and quantitate the forward-going ($dI_{W^+}$, due to $P_{Ao}$) and backward-going waves ($dI_{W^-}$, undoubtedly a function of intramyocardial pressure and elastance), and their net effect ($dI_W$), which governs velocity directly.

*Effects of LV relaxation on coronary blood pressure and velocity.* Consistent with the concept that changes in LV elastance are similarly reflected in all of its cavities, luminal and vascular (16), LV relaxation would appear to generate "aspirating forces" (34), which are manifest as forward- and backward-going expansion waves. With respect to the LV lumen, relaxation decelerates the column of aortic blood and decreases $P_{Ao}$; this effect is observed in the coronary artery as a forward expansion wave. With respect to the intramural LV vasculature, relaxation decreases microvascular compression; this effect is observed in the coronary artery as a backward expansion wave. Thus, in the coronary artery, the effects of LV relaxation are seen as forward (via the aorta) and backward (via the vasculature) expansion waves. Closure of the aortic valve generated forward and backward compression waves that interrupted the expansion waves that preceded and followed them. (Presumably the forward compression wave generated by aortic closure was primary, and the backward compression wave generated by positive reflection from "closed-end" microcirculatory reflection sites was secondary.) Consistent with the fact that $dI_W$ was positive during this interval (i.e.,

the forward compression wave was larger than the backward wave), velocity increased. After these paired forward and backward compression waves, relaxation again dominated as manifest by paired (i.e., forward and backward) expansion waves. Thus LV relaxation seems to become manifest as triplets of forward and backward waves.

At the beginning of relaxation, the effects of forward and backward expansion waves decreased coronary pressure, but they had different effects on coronary velocity: the forward expansion wave decreased blood velocity, but the backward expansion wave increased velocity. The net effect of these two waves determined flow velocity. Because $dI_{W^+} > dI_{W^-}$, $dI_W > 0$, the forward expansion wave dominated and coronary blood velocity decreased during this interval.

During the latter part of isovolumic relaxation, the relaxing myocardium generated a backward expansion wave that was greater than the forward wave. As the result, the dominant backward expansion wave ($dI_W < 0$; Fig. 6) increased coronary velocity and decreased coronary pressure. Although the early and late backward expansion waves were similar in magnitude, the late forward expansion wave was smaller, consistent with the fact that the closed aortic valve prevented $P_{Ao}$ from falling as fast as $P_{LV}$. The phenomena of LV relaxation require further study.

*Limitation of the study.* As described in METHODS, because the caliber of the circumflex branch did not admit a catheter with a lumen, the absolute value of the high-fidelity $P_{LCx}$ could not be ascertained by comparison to the output of an external transducer. Because $dI_{W^+}$ and $dI_{W^-}$ were negligible in the coronary artery during the interval preceding end diastole, we assumed that $P_{LCx}$ was equal to $P_{Ao}$, and we therefore matched $P_{LCx}$ to $P_{Ao}$ at end diastole. (This assumption was supported by measurements using an open catheter.) To the degree that this procedure was not accurate or appropriate, the values of $\Delta P_X$ might have been over- or underestimated. However, the slopes of $P_{Ao}$ and $P_{LCx}$ do not depend on the absolute values of $P_{Ao}$ and $P_{LCx}$, and the facts that the two pressures diverged and diverged more rapidly after paired pacing are unequivocal.

*Conclusions.* WIA elucidates the dynamics of coronary blood flow and identifies and quantitates the upstream (i.e., aortic) and downstream (i.e., coronary vascular) effects. During isovolumic contraction, distal coronary pressure exceeds $P_{Ao}$ and coronary velocity decreases, caused by a backward-going compression wave that is generated by increasing myocardial elastance, effects that are magnified when LV contractility is augmented by paired pacing. During LV relaxation, decreasing elastance appears to generate forward-going (via the aorta) and backward-going (via the coronary vasculature) expansion waves. Thus, during contraction, upstream and downstream effects produce compression waves, and, during relaxation, upstream and downstream effects produce expansion waves. Coronary pressure and velocity depend on the balance of these effects.

We acknowledge the excellent technical support provided by Cheryl Meek, Gerald Groves, and Rozsa Sas. We also thank Drs. N. M. Anderson and I. Belenkie for helpful comments and criticisms.

Y.-H. Sun received a doctoral research scholarship from the Medical Research Council of Canada (Ottawa). T. J. Anderson is a Heritage Medical Clinical Investigator and J. V. Tyberg is a Heritage Medical Scientist of the Alberta Heritage Foundation for Medical Research (Edmonton). The study was supported by Grants-in-Aid from the Heart and Stroke Foundation of Alberta (Calgary) to T. J. Anderson and J. V. Tyberg.

## REFERENCES

1. **Armour JA and Klassen GA.** Epicardial coronary venous pressure. *Can J Physiol Pharmacol* 59: 1250–1259, 1981.
2. **Arts T, Kruger RTI, van Greven W, Lambregts JAC, and Reneman RS.** Propagation velocity and reflection of pressure waves in the canine coronary artery. *Am J Physiol Heart Circ Physiol* 237: H469–H474, 1979.
3. **Berne RM and Levy MN.** *Cardiovascular Physiology*. St. Louis, MO: Mosby, 1986, p. 200.
4. **Chilian WM and Marcus ML.** Phasic coronary blood flow velocity in intramural and epicardial coronary arteries. *Circ Res* 50: 775–781, 1982.
5. **Downey JM, Downey HF, and Kirk ES.** Effect of myocardial strains on coronary blood flow. *Circ Res* 34: 286–292, 1974.
6. **Downey JM and Kirk ES.** Distribution of the coronary blood flow across the canine heart wall during systole. *Circ Res* 34: 251–257, 1974.
7. **Downey JM and Kirk ES.** Inhibition of coronary blood flow by a vascular waterfall mechanism. *Circ Res* 36: 753–763, 1975.
8. **Flynn AE, Coggins DL, Goto M, Aldea GS, Austin RE, Doucette JW, Husseini W, and Hoffman JIE.** Does systolic subepicardial perfusion come from retrograde subendocardial flow? *Am J Physiol Heart Circ Physiol* 262: H1759–H1769, 1992.
9. **Gow B, Schonfeld D, and Patel DJ.** The dynamic elastic properties of the canine left circumflex coronary artery. *J Biomech* 7: 389–395, 1974.
10. **Grant DA, Hollander E, Skuza EM, and Fauchere J-C.** Interactions between the right ventricle and pulmonary vasculature in the fetus. *J Appl Physiol* 87: 1637–1643, 1999.
11. **Hollander EH.** *Wave-Intensity Analysis of Pulmonary Arterial Blood Flow in Anesthetized Dogs* (Ph.D. thesis). Calgary, AB, Canada: University of Calgary, 1998.
12. **Jones CJH, Parker KH, Hughes R, and Sheridan DJ.** Nonlinearity of human arterial pulse wave transmission. *J Biomech Eng* 114: 10–14, 1992.
13. **Jones CJH, Sugawara M, Davies RH, Kondoh Y, Uchida K, and Parker KH.** Arterial wave intensity: physical meaning and physiological significance. In: *Recent Progress in Cardiovascular Mechanics*, edited by Hosoda S, Yaginuma T, Sugawara M, Taylor MG, and Caro CG. Chur, Switzerland: Harwood, 1994, p. 129–148.
14. **Kajiya F, Goto M, Yada T, Ogasawara Y, and Tsujioka K.** Mechanics of intramural blood vessels of the beating heart. In: *Biological Flows*, edited by Jaffrin MY and Caro CG. New York: Plenum, 1995, p. 255–265.
15. **Klassen GA and Zborowska-Sluis DT.** The effect of myocardial force on coronary transmural flow distribution. *Cardiovasc Res* 13: 365–369, 1979.
16. **Krams R, Sipkema P, and Westerhof N.** Varying elastance concept may explain coronary systolic flow impediment. *Am J Physiol Heart Circ Physiol* 257: H1471–H1479, 1989.
17. **Krams R, Sipkema P, Zegers J, and Westerhof N.** Contractility is the main determinant of coronary systolic flow impediment. *Am J Physiol Heart Circ Physiol* 257: H1936–H1944, 1989.
18. **Krams R, van Haelst ACTA, Sipkema P, and Westerhof N.** Can coronary systolic-diastolic flow differences be predicted by left ventricular pressure or time-varying intramyocardial elastance? *Basic Res Cardiol* 84: 149–159, 1989.
19. **Lighthill MJ.** *Waves in Fluids*. Cambridge, UK: Cambridge University Press, 1978, p. 106.
20. **Pagliaro P, Paolocci N, Isoda T, Saavedra WF, Sunagawa G, and Kass DA.** Reversal of glibenclamide-induced coronary

vasoconstriction by enhanced perfusion pulsatility: possible role for nitric oxide. *Cardiovasc Res* 45: 1001–1009, 2000.
21. **Pagliaro P, Senzaki H, Paolocci N, Isoda T, Sunagawa G, Recchia FA, and Kass DA.** Specificity of synergistic coronary flow enhancement by adenosine and pulsatile perfusion in the dog. *J Physiol (Lond)* 520: 271–280, 1999.
22. **Parker KH and Jones CJH.** Forward and backward running waves in the arteries: analysis using the method of characteristics. *J Biomech Eng* 112: 322–326, 1990.
23. **Parker KH, Jones CJH, Dawson JR, and Gibson DG.** What stops the flow of blood from the heart? *Heart Vessels* 4: 241–245, 1988.
24. **Recchia FA, Senzaki H, Saeki A, Byrne BJ, and Kass DA.** Pulse pressure-related changes in coronary flow in vivo are modulated by nitric oxide and adenosine. *Circ Res* 79: 849–856, 1996.
25. **Ross, J Jr, Sonnenblick EH, Kaiser GA, Frommer PL, and Braunwald E.** Electroaugmentation of ventricular performance and oxygen consumption by repetitive application of paired electrical stimuli. *Circ Res* 16: 332–342, 1965.
26. **Rumberger JA, Nerem RM, and Muir WW III.** Coronary artery pressure development and wave transmission characteristics in the horse. *Cardiovasc Res* 13: 413–419, 1979.
27. **Sabiston, DC Jr and Gregg DE.** Effect of cardiac contraction on coronary blood flow. *Circulation* 15: 14–20, 1957.
28. **Sagawa K, Suga H, Shoukas AA, and Bakalar KM.** End-systolic pressure-volume ratio: a new index of ventricular contractility. *Am J Cardiol* 40: 748–753, 1977.
29. **Smiseth OA, Thompson CR, Lohavanichbutr K, Abel JG, Miyagishima RT, Lichtenstein SV, and Bowering J.** The pulmonary venous systolic flow pulse—its origin and relationship to left atrial pressure. *J Am Coll Cardiol* 34: 802–809, 1999.
30. **Spaan JAE, Breuls PW, and Laird JD.** Diastolic-systolic coronary flow differences are caused by intramyocardial pump action in the anaesthetized dog. *Circ Res* 49: 584–593, 1981.
31. **Suga H and Sagawa K.** Instantaneous pressure-volume relationships and their ratio in the excised, supported canine left ventricle. *Circ Res* 35: 117–126, 1974.
32. **Sun Y-H, Anderson TJ, and Tyberg JV.** Effects of coronary vascular tone and myocardial compression on systolic coronary flow reduction (Abstract). *J Cardiovasc Diagn Proc* 13: 288, 1996.
33. **Van Huis GA, Sipkema P, and Westerhof N.** Coronary input impedance during cardiac cycle as determined by impulse response method. *Am J Physiol Heart Circ Physiol* 253: H317–H324, 1987.
34. **Wiggers CJ.** Cardiac mechanisms that limit operation of ventricular suction. *Science* 126: 12–37, 1957.